T17-13	Disruptions and runaways
	D3 Simulate the conditions under which RE are formed. **D4 Propose operational methods for control the runaway beam in the JET chamber.**

1. Gamma-ray Camera at JET

The Gamma-ray Camera (GC) is one of the diagnostics system used at JET. It consists of 19 scintillator detectors, dedicated electronic devices and a data acquisition system. In each aluminum capsule a scintillator connected to a photomultiplier is fixed. Before the upgrade of GC, CsI scintillators and PIN-diode photomultipliers were used. These detectors are replaced by $LaBr_3$ scintillator and the MPPC device which is used as a photomultiplier due to project requirements. In the horizontal and vertical parts of GC 10 and 9 detectors are placed, respectively. The schematic of the GC (left) and a capsule (right) is shown in Fig. 1.

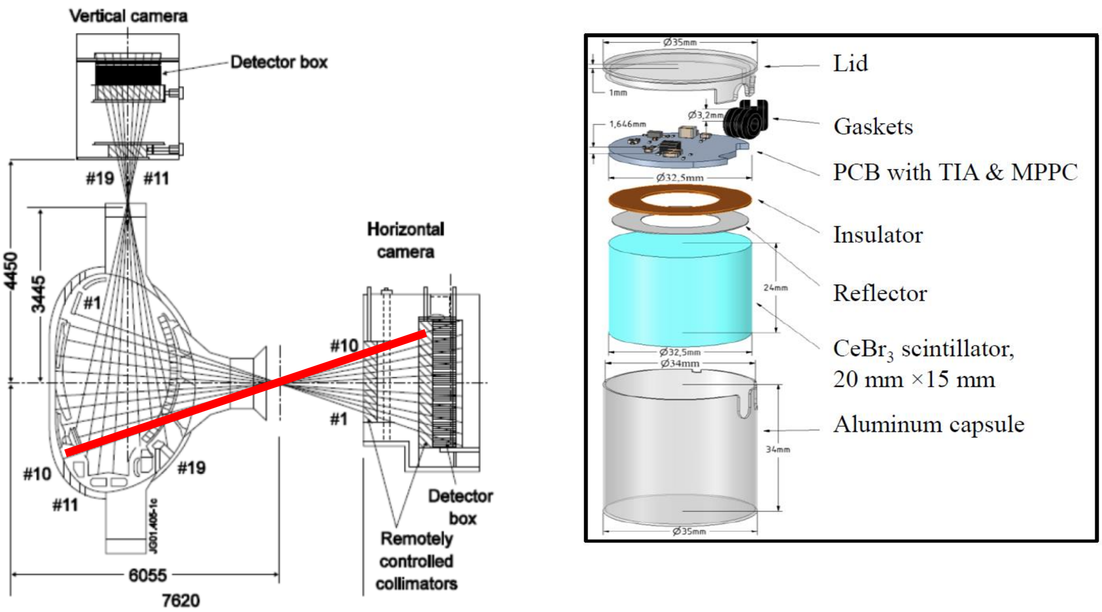

Fig. 1. Schematic of the JET Gamma-ray Camera (left) and a capsule with 20×15 mm $CeBr_3$-based detector (right).

During the test phase in May 2015 a scintillator $CeBr_3$ with a MPPC array was placed in the channel #10 which is a part of the Horizontal Camera (HC). Data registered with this detector are analyzed in this work.

The electronic system consists of the FilterBox@NCBJ and MTCD@NCBJ devices. The MTCD@NCBJ device provides the power and the temperature compensation. The FilterBox@NCBJ is used for communication between the MTCD@NCBJ and the temperature sensors placed on the detectors.

The new Data Acquisition System (DAQ) was implemented and installed by the IST group.

2. Energy calibration

The energy calibration measurements were performed on 20th July, 2016. There was a series of one-hour measurements with a ^{22}Na source, emitting 511 and 1274 keV. The energy calibration is obtained from a formula:

$$\text{Energy (keV)} = (3.34 \cdot \text{channel} + 137).$$

3. Analysis of raw data for runaway electron (RE) production from JET Gamma-ray Camera

During analysis we extract time and energy for each event during a shot:

- read time and amplitude data from a DAQ file,
- perform energy calibration,
- use a proper code depending on a scintillator type (CsI or $CeBr_3$/$LaBr_3$:Ce) to obtain an amplitude and to find single (not pile-up) and pile-up events,
- apply a code AU_main to unfold pile-up events,
- split events into two parts: with energy ≤520 keV and >520 keV. With such a value, all events from a 511 keV peak, corresponding to an annihilation process, are only in the lower part,
- plot two spectra:
  - number of counts vs. channel, corresponding to energy (if a reliable energy calibration is available),
  - number of counts vs. time for each energy range as well as for a full energy range,
- all results of the analysis are saved in text files.

3.1. Description of the AU_main program used for data analysis

The AU_main program to analyze data from Gamma Camera (GC) is written in C++ language. It consists of classes:
Events
ReadBin
PileupFilter
Analysis
The DAQ time to start acquisition is provided by the JET absolute time (CTTS clock and trigger) with the precision of 1 MHz. The data file is composed of events (PWIDTH samples of 16-bit). Each event corresponds to: an occurrence time (64-bit) which is the first 4 samples and a pulse amplitude which is (PWIDTH-4) samples.

There are three structures implemented due to three types of saved data:
struct event_CeBr_1024{ uint64_t time; int16_t amplitude[1024]; };
struct event_CeBr_512{ uint64_t time; int16_t amplitude[512];};
struct event_CsI{ int32_t amplitude; uint32_t time; };

The class *Events* is a template of a vector which contains such information about signals as a time and an amplitude. This object is created by the function *readEventsFromBin()* which is a part of the class *ReadBin*.

The class *ReadBin* is used to read a binary output file which is generated by DAQ dedicated for the GC. This class is able to distinguish three types of events:

1. events collected with CsI scintillatrs,
2. events collected with a new $CeBr_3$ scintillator and an old DAQ
3. events with a new crystal $LaBr_3$:Ce and a new DAQ. In this case, the *ReadBin* class creates the *PileupFilter* object to unfold pile-up events. The function *readEventsFromBin()* returns a vector of *Events* objects which is sent to the object *Analysis*.

The class *PileupFilter* is used to unfold pile-up signals. Two types of pile-up events are considered:

- a signal length is longer than the data acquisition time (including the detector, MPPC and electronics resolution time),
- a signal rate is relatively high.

In each of these two signal types, more than one signal is registered in an event, see Fig. 2.

For low rates, a **single signal** comes: ***time*** and ***amplitude*** are saved.	For high rates, a **pile-up** event comes: after pile-up decomposition ***time*** and **amplitude** are saved for each component signal.

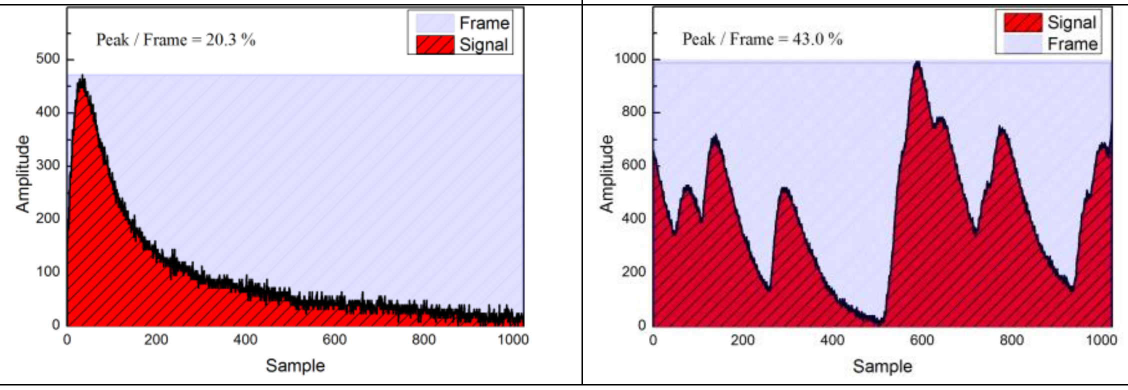

Fig. 2. Signals registered in the GC detectors: left – single event, right – pile-up event.

<u>In case of a single event</u>, a signal shape is described by a formula:

$$f(t) = a \cdot (\exp(-t/\tau_1) - \exp(-t/\tau_2)), \qquad \text{Eq. (1)}$$

where a is a constant, t is time, τ_1 and τ_2 are time constants dependent on the detector. A time length and an amplitude of this signal can be easily calculated, see Fig. 3. In addition, it is possible to obtain a pattern of such a single signal.

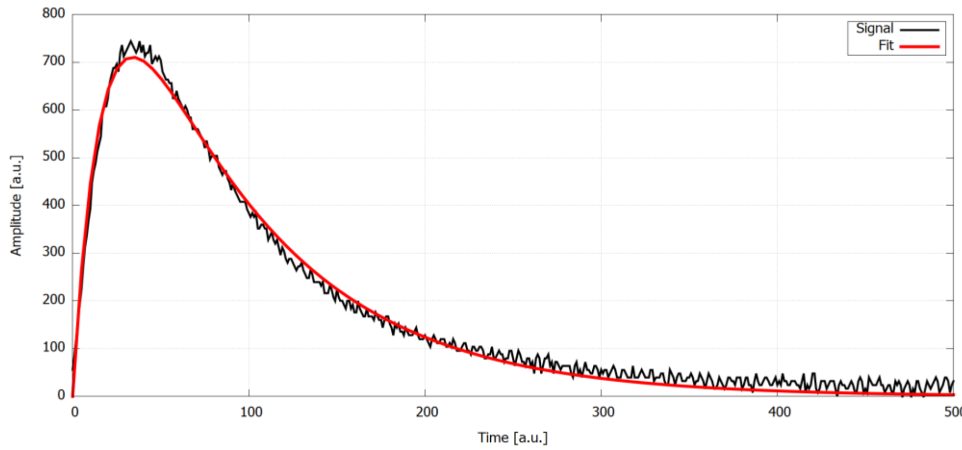

Fig. 3. Fit, described by Eq. (1), to a measured signal: a= -1333, τ_1=16.99, τ_2=84.26.

<u>In case of a pile-up event</u>, more than one consists of more than signal is registered. So, a more complicated special formula is needed to obtain both time and amplitude of a signal. This is realized by the class *PileupFilter*.

When a pile-up event is registered, it is compared to the single signal pattern and a pile-up event is decomposed into single ones. Such extracted new single signals are saved. For each event, a pile-up discriminator value, equal to a ratio of an area below a signal to a rectangular frame area based on a signal amplitude and a number of samples, was calculated, see blue rectangle in Fig. 2.

The *Analysis* object loads the *Event* object and builds an energy spectrum and calculates how many events were recorded during a shot, especially for energy ≤520 keV and >520 keV.

The flowchart of the analysis program is shown in Fig. 3.

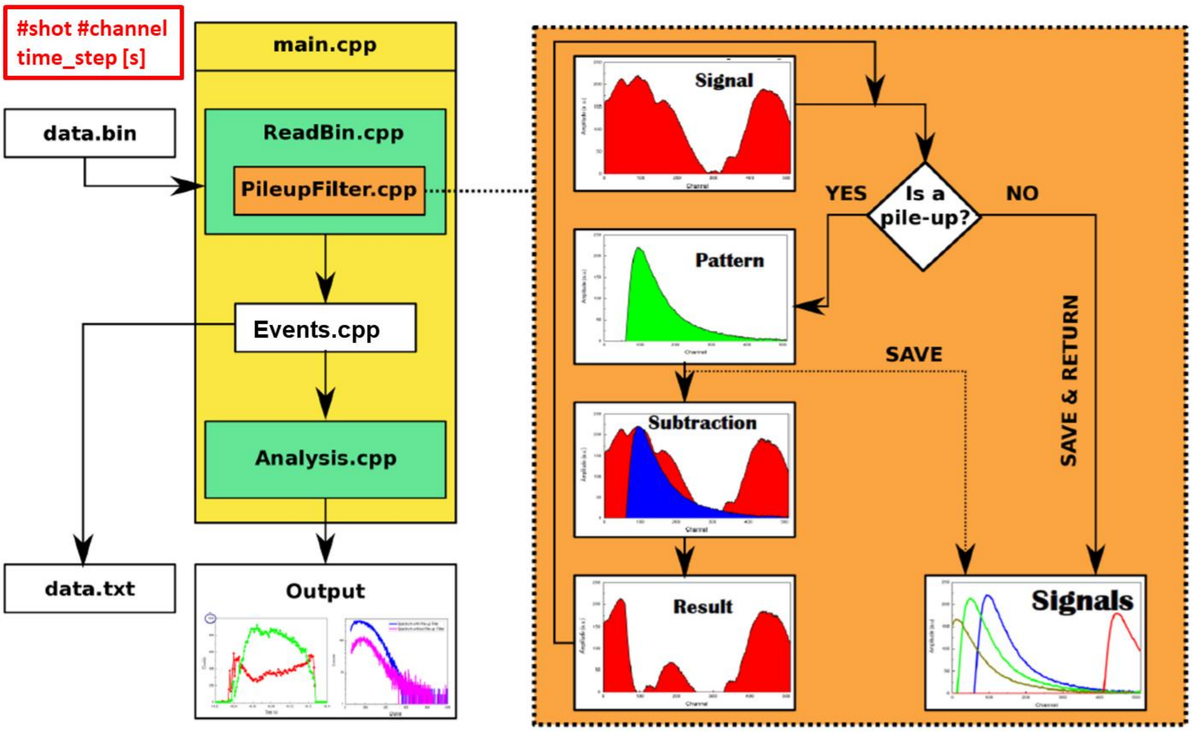

Fig. 3. Flowchart of the analysis program.

Three input parameters should be supplied by the user:

1. shot number,
2. detector channel number from 1 to 19: 1-10 for the horizontal camera and 11-19 for the vertical one,
3. time step in seconds as demanded by the user.

Staring the AU_main program: ***./AU_main 92449 10 0.001***

A *ReadBin* object calls *readFromFile()* which uses a *PileupFilter* object and returns an *Event* object which collects all events. The *Event* object, with all collected events, is then relayed to an *Analysis* object, calling dedicated analysis methods.

The output of the AU_main analysis program contains the following four text files of the same structure: channel, energy in keV, counts

1. Analysis_RE_Spectrum.dat
2. Analysis_RE_low.dat for the low energy range ≤520 keV
3. Analysis_RE_high.dat for high energy range >520 keV
4. Analysis_RE_full.dat for a full energy range

The AU_main program is prepared for a Linux operating system and extensively tested on JAC computers.

3.2. Comparison of CsI and $CeBr_3$ detector performance

CsI scintillators have slower response time and lower efficiency in comparison to CeBr3 scintillators. In Fig. 4 a distribution of counts vs. time from a shot #91069 is presented with a time step equal to 0.001 second (input to the AU_main program).

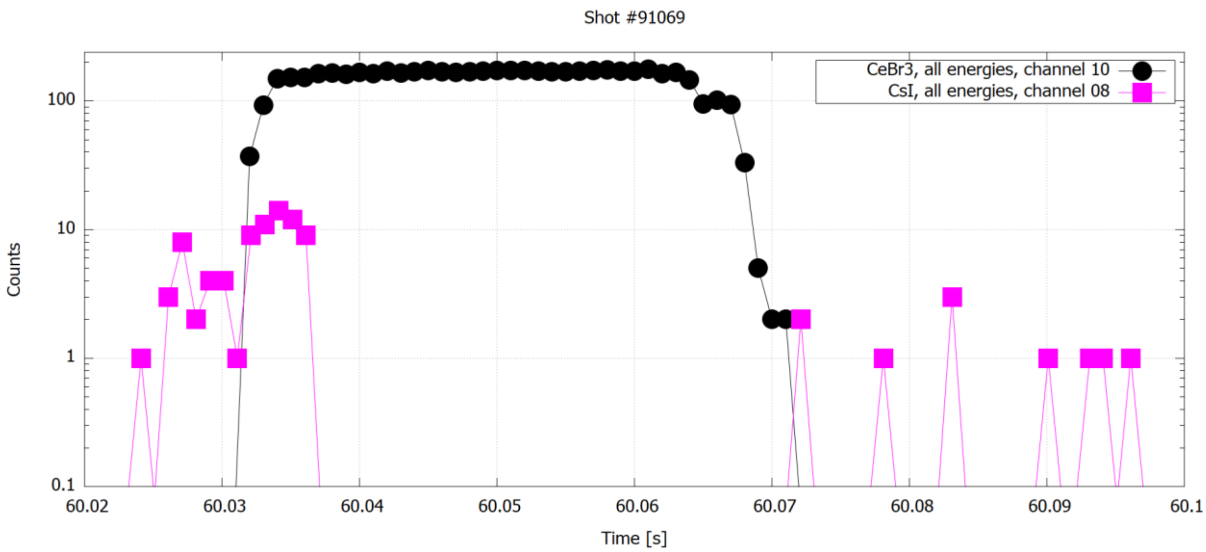

Fig. 4. Comparison between number of counts obtained with CsI (magenta triangles) and $CeBr_3$ (black dots) detectors.

No signal with old CsI is registered during a disruption. This effect can be related to a higher dead time of the CsI detector which was not able to register higher count rates. This effect was observed in each channel with old CsI-based detectors, i.e. from channel #1 to #8 in a horizontal part and from #11 to #19 in a vertical part of the Gamma-ray Camera.

3.3. Analysis of shots from 2016 campaign at JET

The $CeBr_3$-based detector was installed at JET in May 2015 in the channel #10 in the Gamma-ray Camera.

The following parameters were defined for shots, see Fig. 5, :

1. T_{start} - time when gamma events start to be registered in the detector,
2. T_{end} - time when no more gamma events end to be registered in the detector,
3. $\Delta T=T_{end}-T_{start}$ – the duration of a disruption,
4. *N_full* –number of counts during ΔT in the full energy range,
5. *N_low* –number of counts during ΔT in the low energy range,
6. *N_high*–number of counts during ΔT in the high energy range.
7. *N_full/ΔT* – average number of counts during ΔT in the full energy range,
8. *N_low/ΔT* – average number of counts during ΔT in the low energy range,
9. *N_high/ΔT* – average number of counts during ΔT in the high energy range.

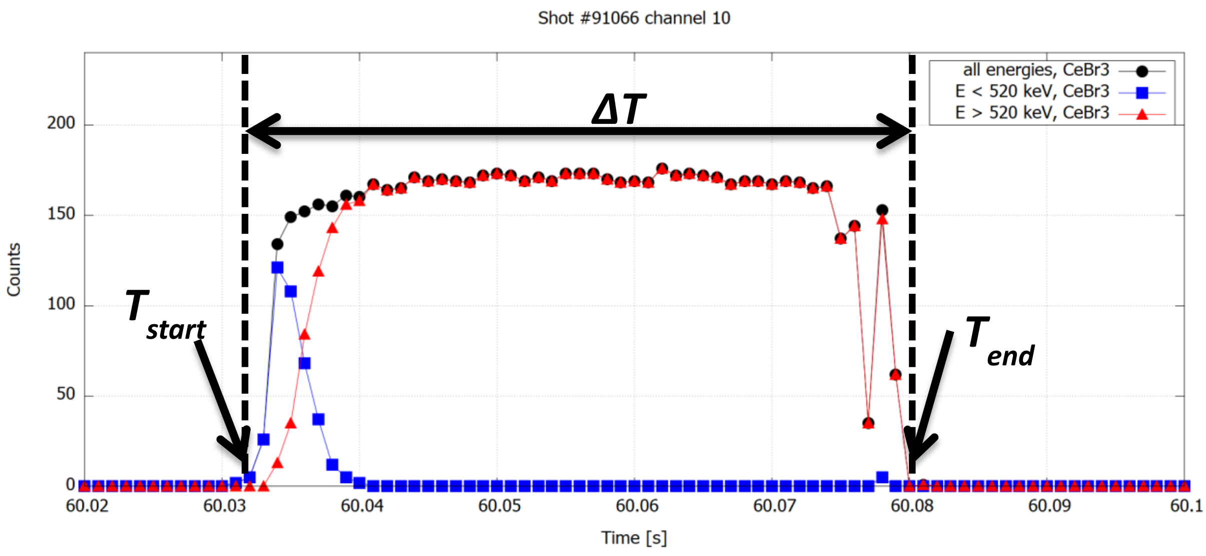

Fig. 5. Definition of parameters defined for each shot.

Results of analysis performed with AU_main program are presented in Table 1.

Below Table 1, distributions plotted for each shot show:

1. amplitude vs. DAQ channel (upper),
2. time distribution of events in the full, low and high energy range (lower).

Table 1. Parameters obtained from analysis for shots from July 2016 (green) and November 2016 (yellow).

shot number	T_{start} [s]	T_{end} [s]	ΔT [ms]	N	N_{low}	N_{high}	$N/\Delta T$ [kcps]	$N_{low}/\Delta T$ [kcps]	$N_{high}/\Delta T$ [kcps]
91066	60.032	60.079	47	7396	395	7001	157	8	149
91067	60.032	60.084	52	8285	245	8040	159	5	155
91068	60.032	60.066	34	4579	262	4317	135	8	127
91069	60.032	60.071	39	5622	351	5271	144	9	135
91071	60.031	60.075	44	6450	429	6021	147	10	137
91076	60.031	60.118	87	12915	298	12617	148	3	145
91077	60.031	60.070	39	5468	477	4991	140	12	128
91079	60.032	60.082	50	6777	322	6455	136	6	129
91081	60.032	60.070	38	5379	473	4906	142	12	129
92448	48.032	48.130	98	107059	35263	71796	1092	360	733
92449	48.028	48.129	101	95139	35232	59907	942	349	593
92454	48.025	48.146	121	116759	51444	65315	965	425	540
92456	48.024	48.100	76	66543	26637	39906	876	350	525
92457	48.023	48.100	77	69236	25222	44014	899	328	572
92458	48.023	48.143	120	120335	46571	73764	1003	388	615
92459	48.034	48.247	213	142589	97251	45338	669	457	213
92460	48.034	48.109	75	62356	31151	31205	831	415	416
92461	48.034	48.091	57	44512	25637	18875	781	450	331

Shot number	Ip/Bt	First gas injection	Second gas injection	Shape	Runaways	Comment
91066	1.0MA/3T	DMV1 7.6 bar 100% Ar	DMV2 45bar 100% Kr. t+50ms.	Limiter	Plateau.	Reference runaway plateau at 1.0 MA pre-disruption current. Late mitigation.

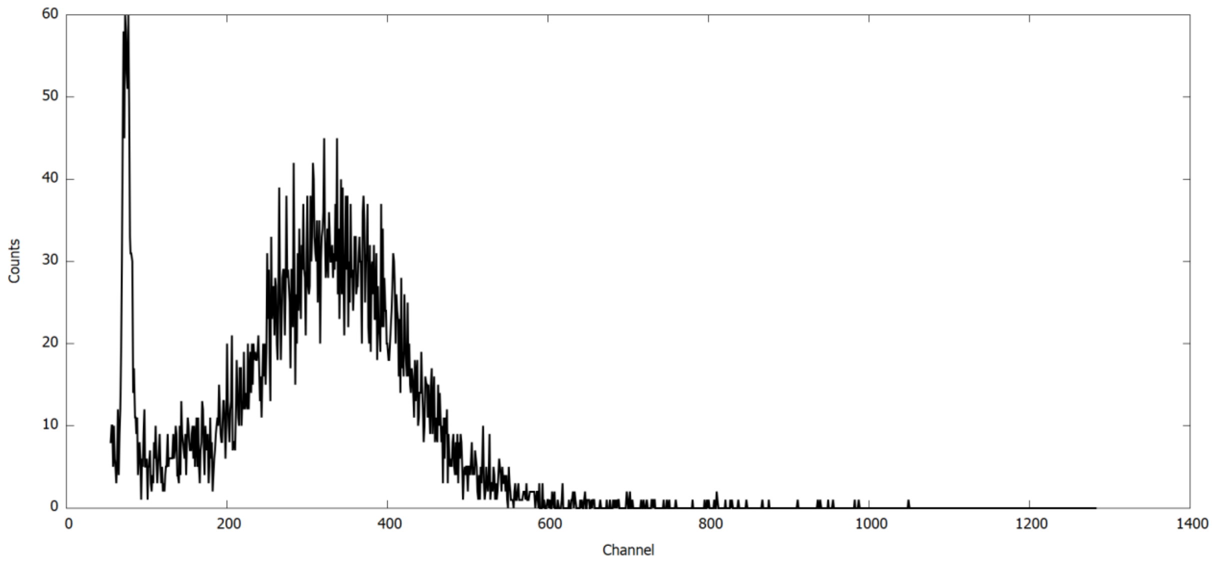

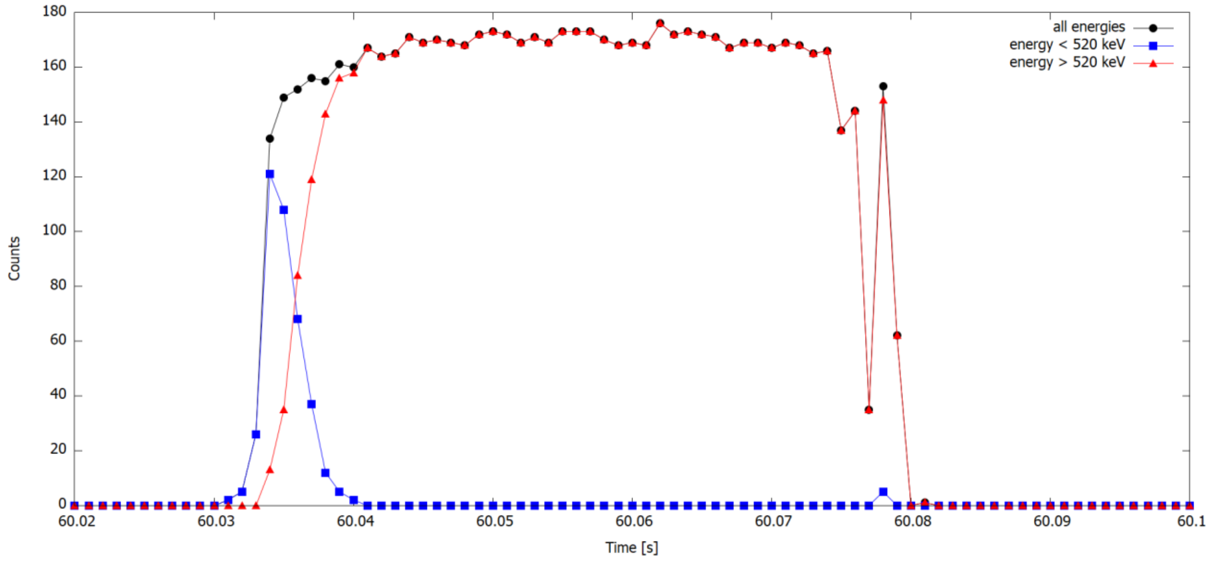

Shot number	Ip/Bt	First gas injection	Second gas injection	Shape	Runaways	Comment
91067	**1.5MA/3T**	**DMV1 7.6 bar 100% Ar**	**DMV2 45bar 100% Kr. t+50ms/t+80ms**	**Limiter**	**Plateau.**	**Reference runaway plateau at 1.5 MA pre-disruption current. Late mitigation**

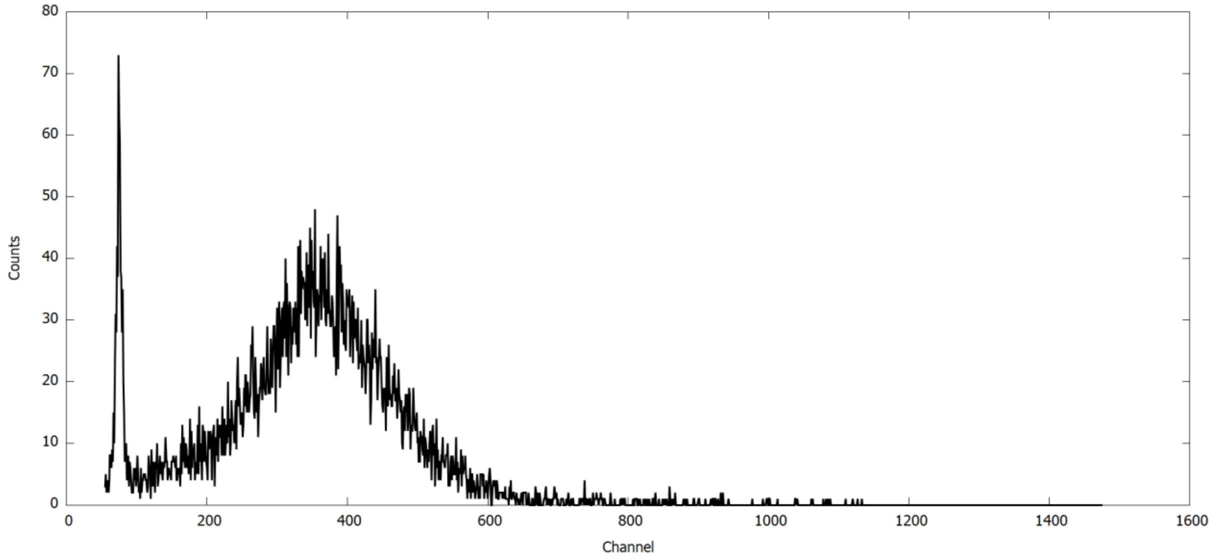

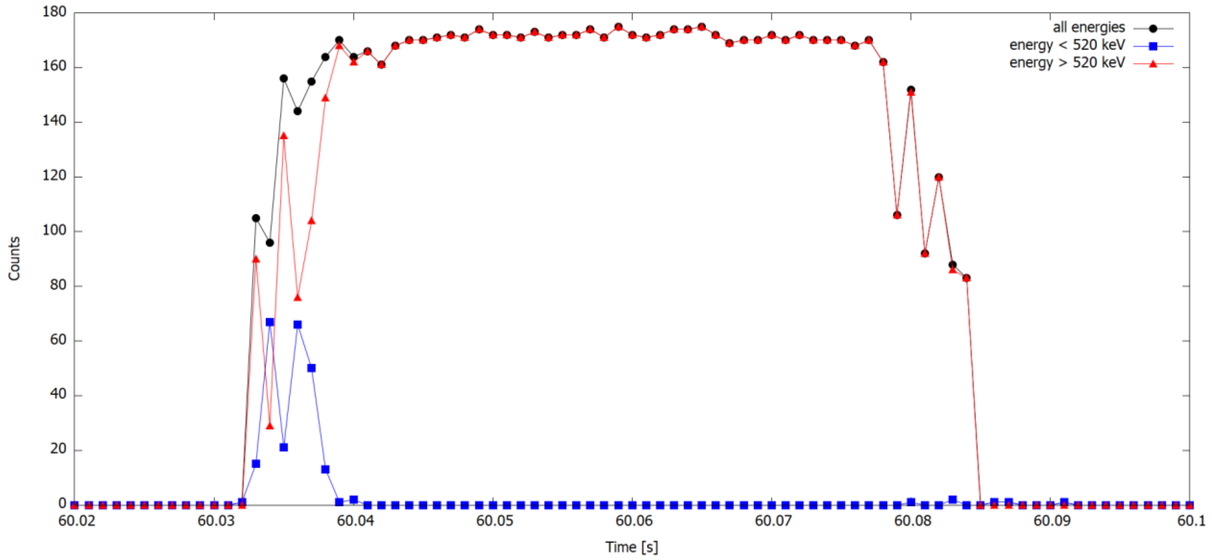

Shot number	Ip/Bt	First gas injection	Second gas injection	Shape	Runaways	Comment
91068	1.5MA/3T	DMV1 7.6 bar 100% Ar	DMV2 45bar 100% Kr. t+28ms.	Limiter	Plateau.	Reference runaway plateau at 1.5 MA pre-disruption current. Early mitigation.

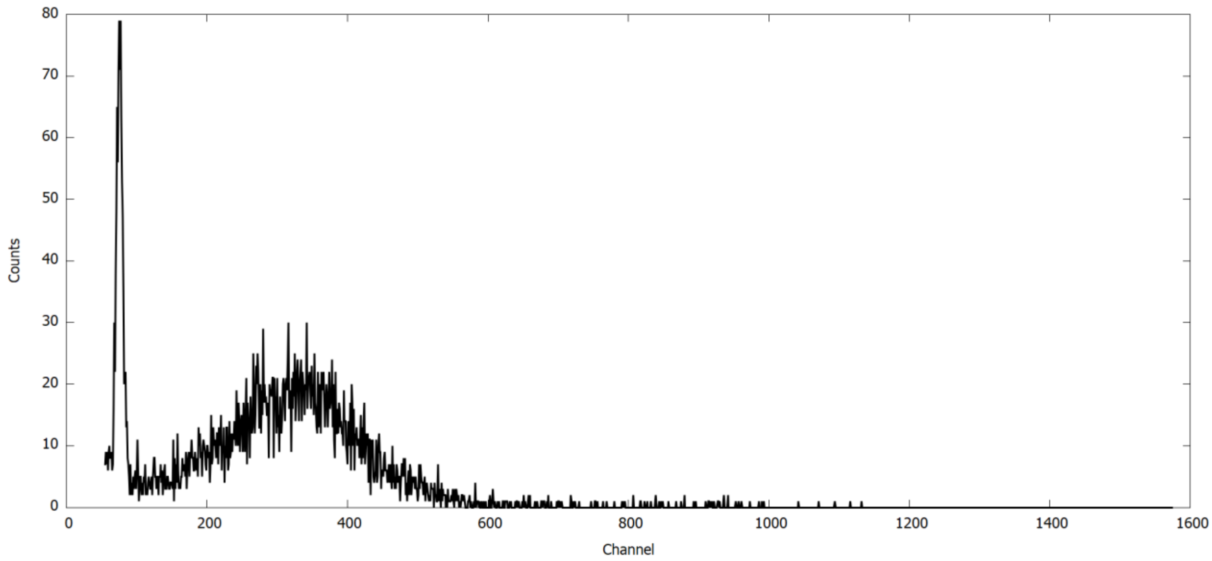

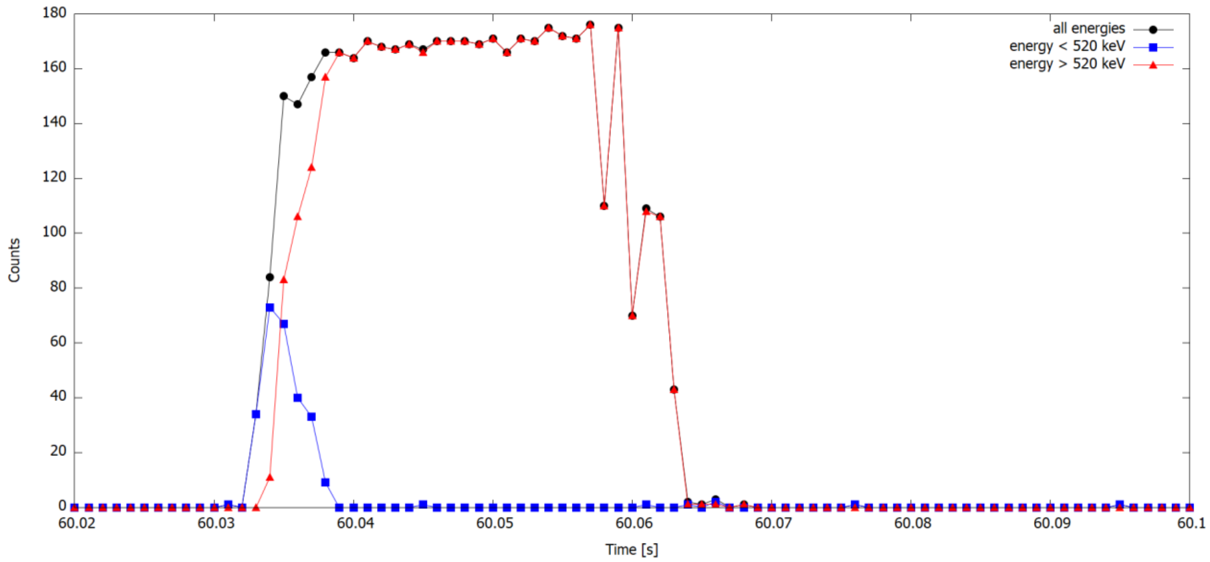

#91069. 1.5MA / 3.0T. DMV1 argon 7.6 bar @60.0s. DMV2 Krypton 45 bar @60.039s. Good! Runaway plateau ends at 60.065s. The end is not exactly in the middle between the 2 previous pulses, but it still goes in the right direction. 700 degC impact on the dump plate from KL7

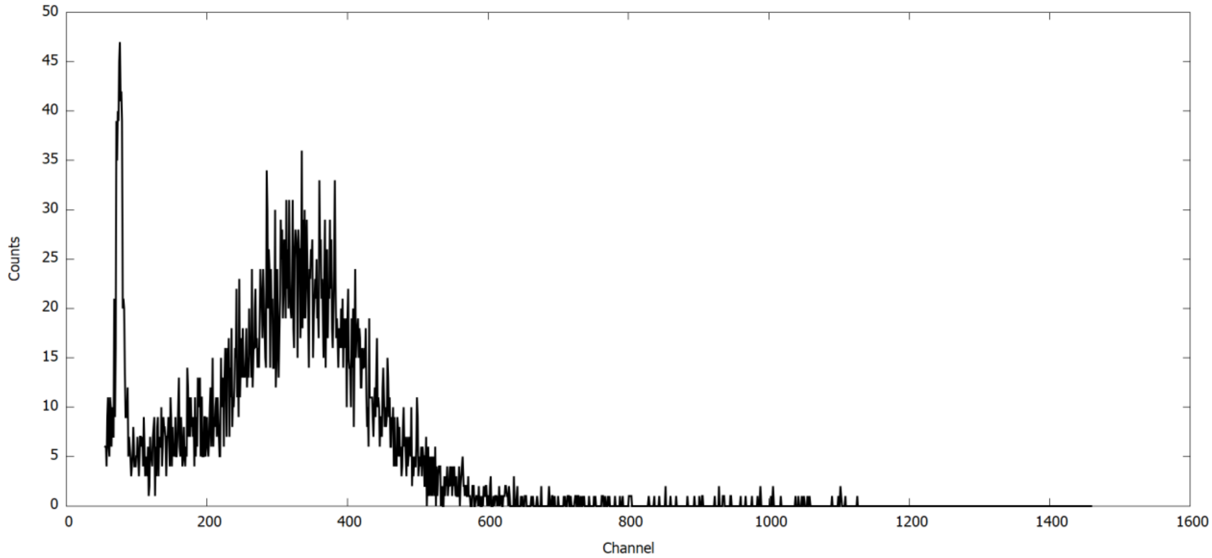

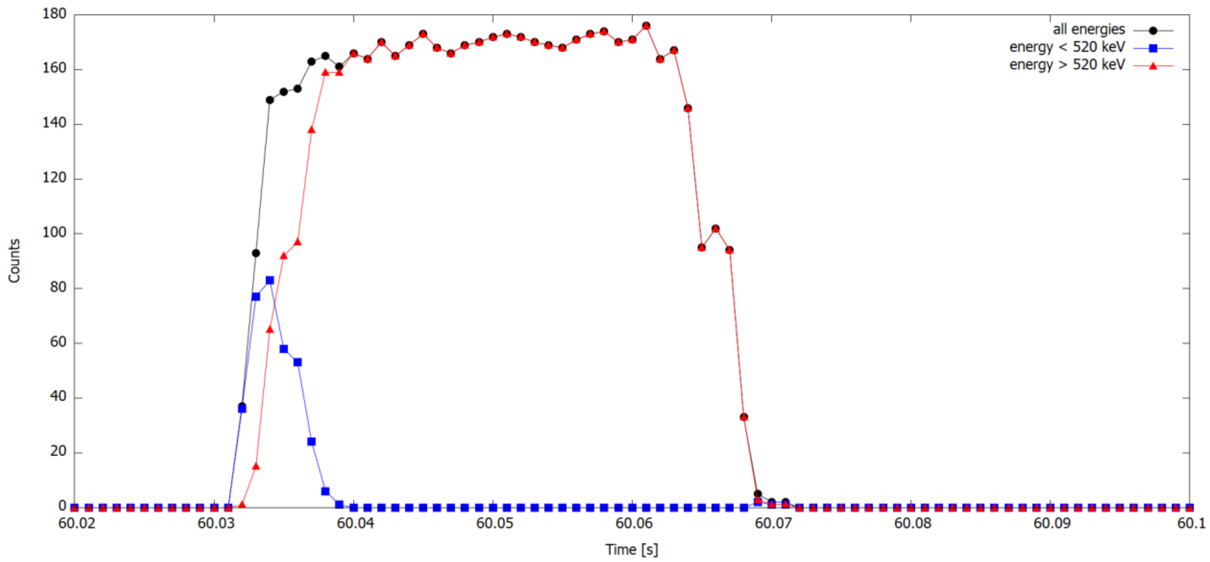

Shot number	Ip/Bt	First gas injection	Second gas injection	Shape	Runaways	Comment
91071	1.5MA/3T	DMV1 7.6 bar 100% Ar	DMV2 45bar 100% Kr. t+50ms/t+80ms	Limiter	Plateau.	Reference runaway plateau at 1.5 MA pre-disruption current. Late mitigation

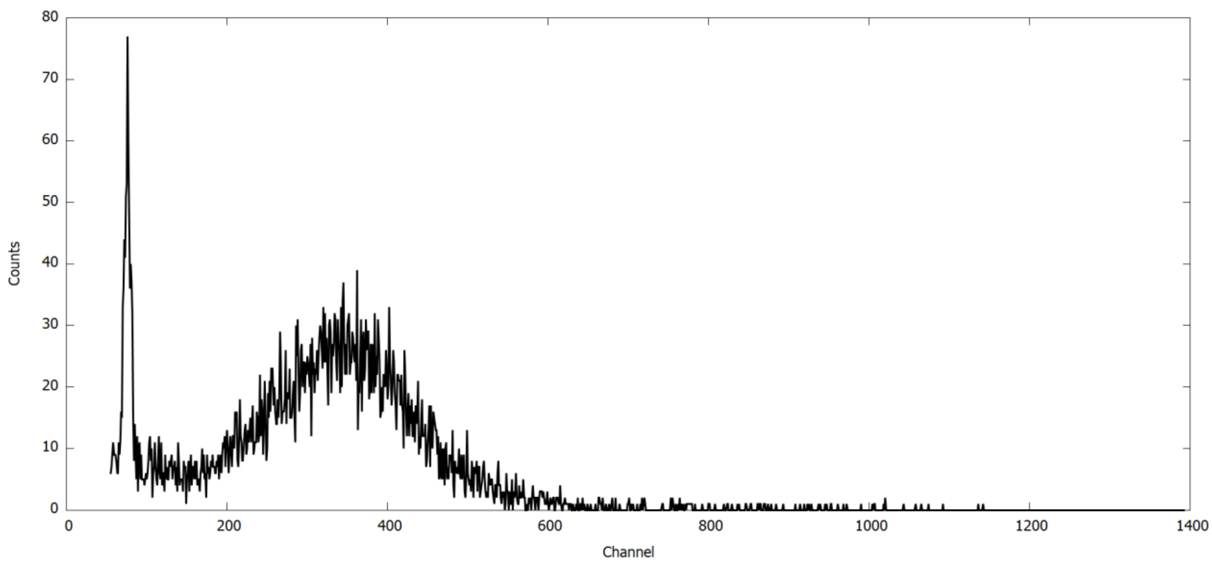

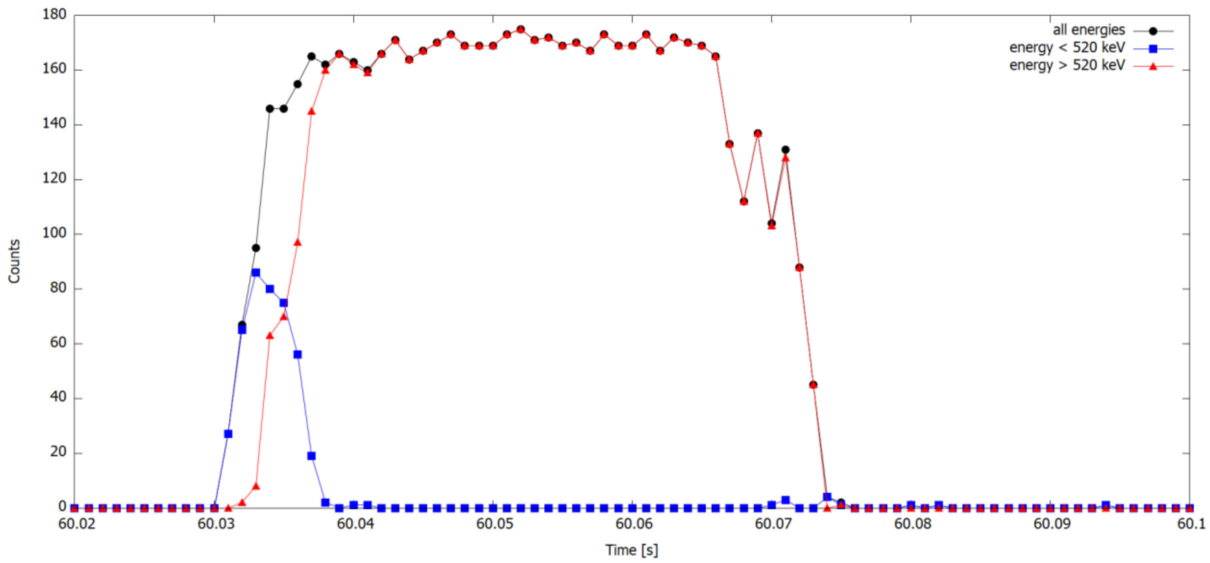

Shot number	Ip/Bt	First gas injection	Second gas injection	Shape	Runaways	Comment
91076	1.5MA/3T	DMV1 7.6 bar 100% Ar	DMV3 39bar 100% Kr. t+28ms.	Limiter	Plateau.	Late-in-the-beam mitigation attempt with DMV3 instead of DMV2.

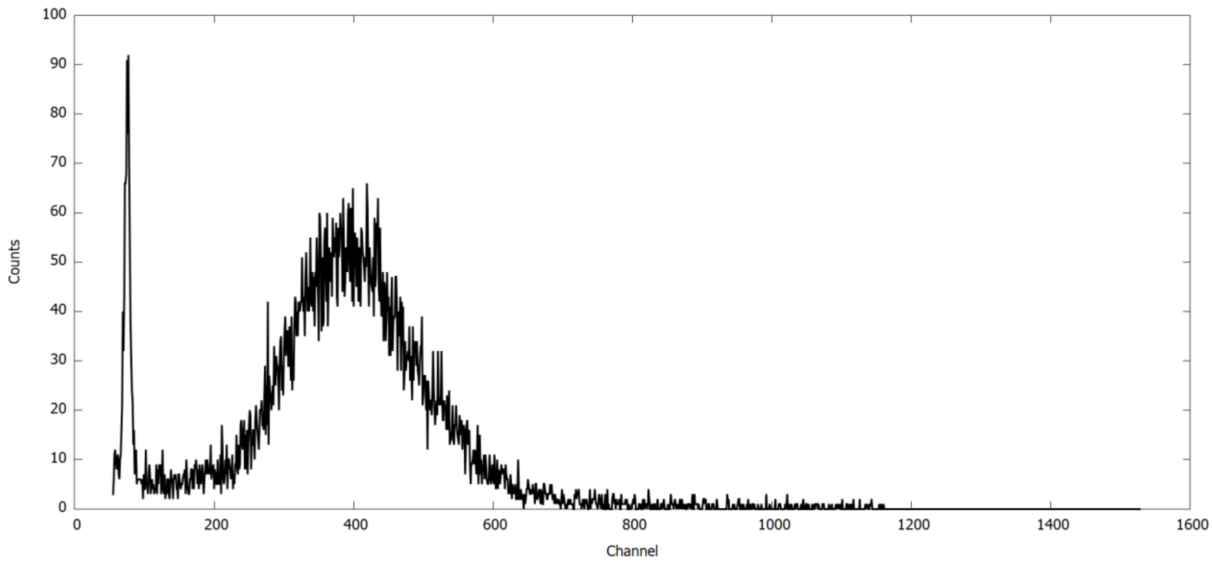

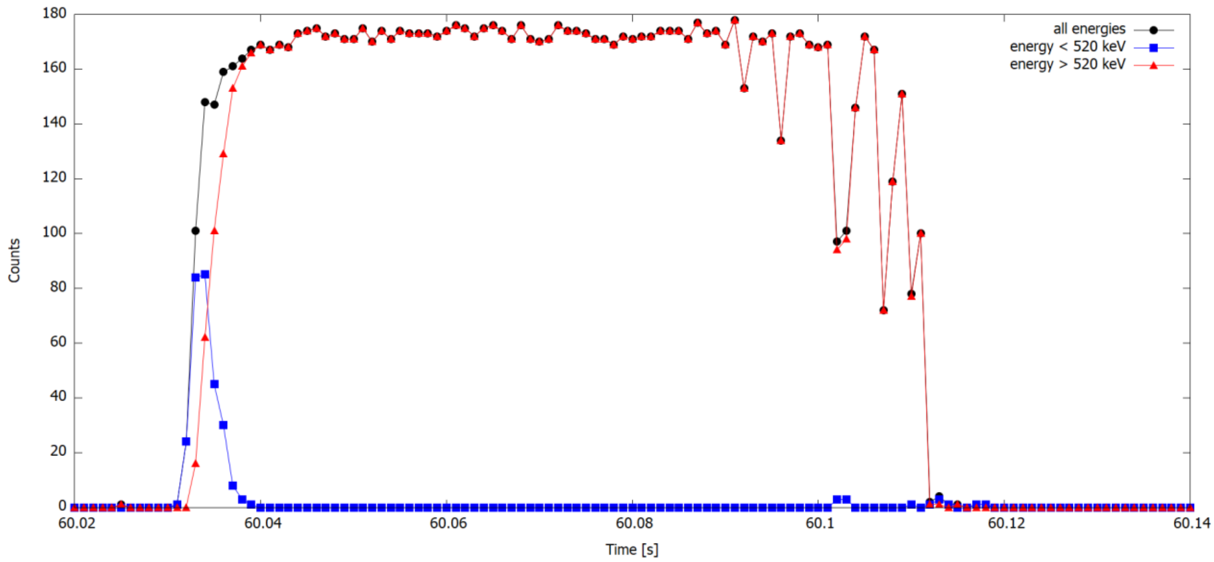

Shot number	Ip/Bt	First gas injection	Second gas injection	Shape	Runaways	Comment
91077	1.5MA/3T	DMV1 7.6 bar 100% Ar	DMV3 39bar 100% Kr. t+28ms.	Limiter	Plateau.	Early-in-the-beam mitigation attempt with DMV3 instead of DMV2.

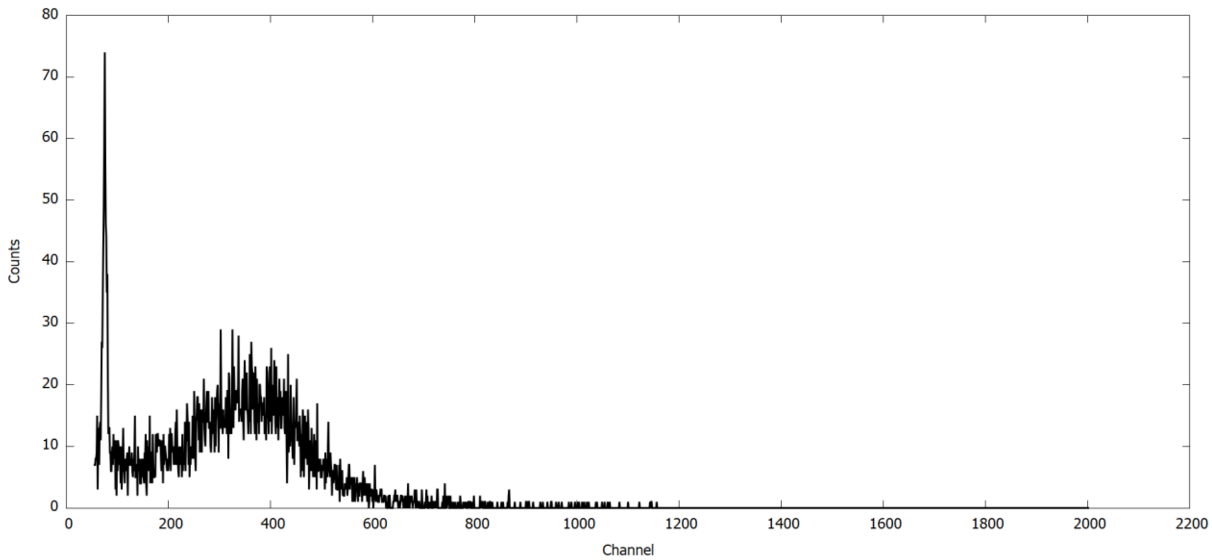

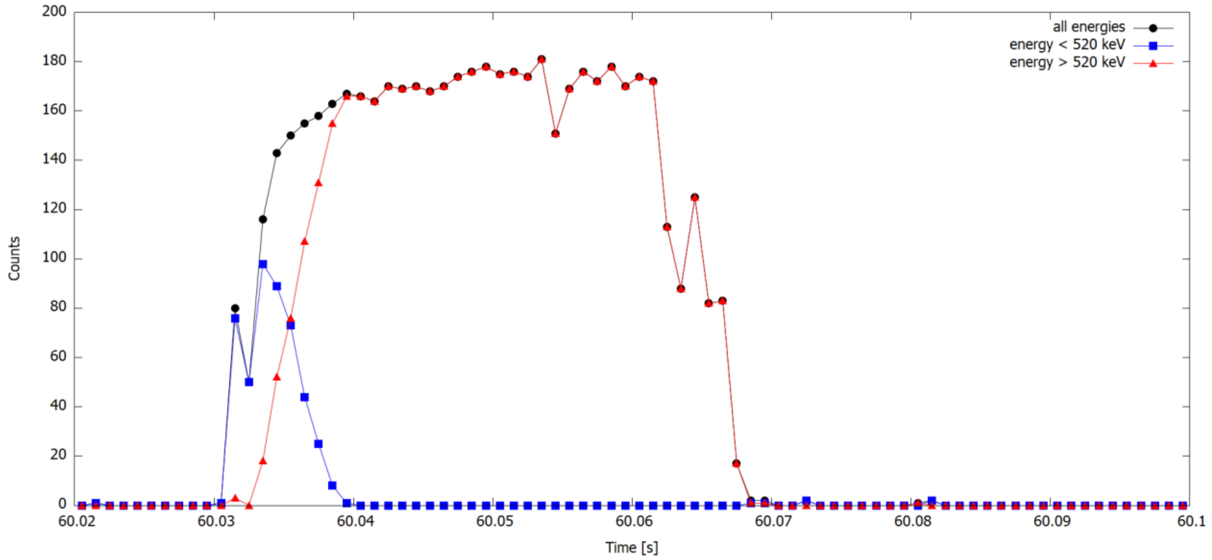

- **#91079**. Repeat #91069 to estimate the variability of the runaway beam. 1.5MA / 3.0T. DMV1 argon 7.6 bar @60.0s. DMV2 Krypton 45 bar @60.039s. Longer than #91069, but starts with a higher initial current. Still, it is longer than #91071 which was not mitigated. Annoying. The scan is now all over the place, and this runaway beam just seems to do what it wants.

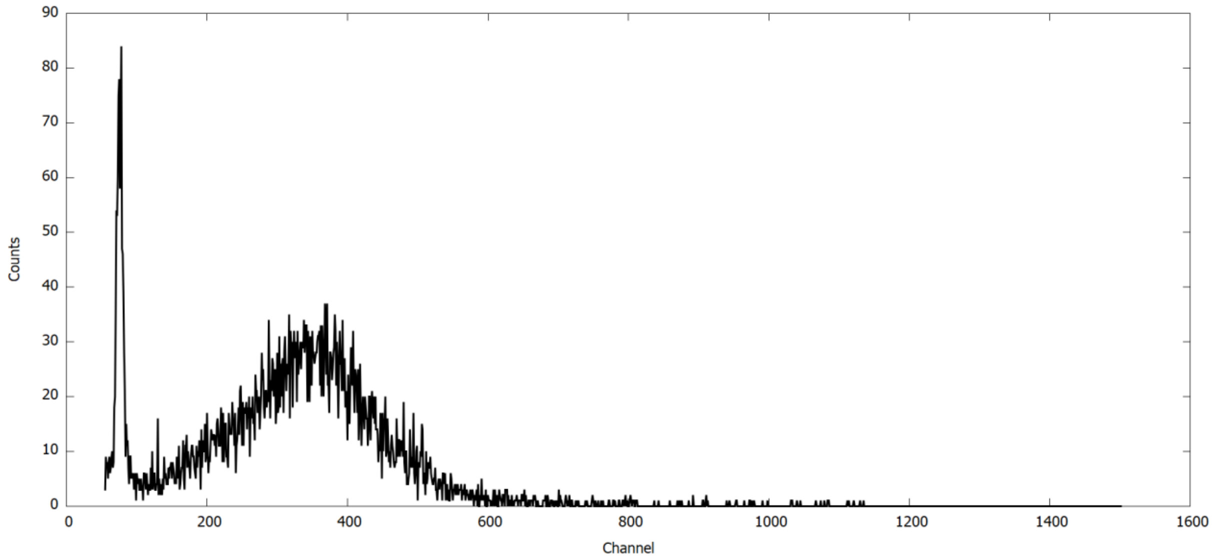

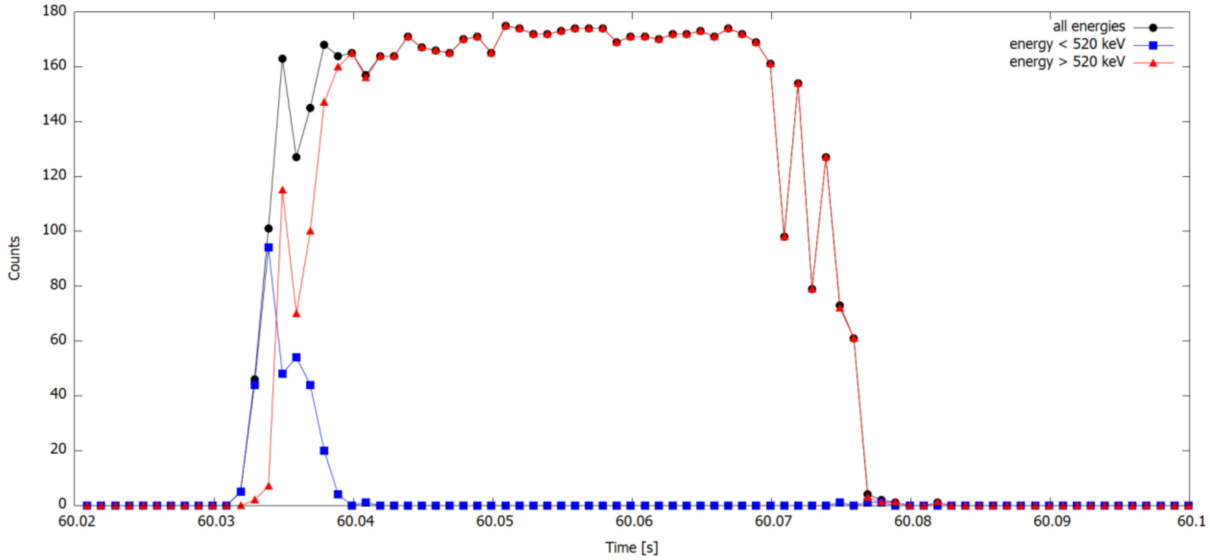

- **#91081**. Repeat #91068 with Neon max pressure. 1.5MA / 3.0T. DMV1 argon 7.6 bar @60.0s. DMV2 Neon 45 bar @60.028s. Beam ends around 60.065s. Longer than #91068, but not enough to conclude that Neon is less efficient than krypton. And another unconclusive pulse...

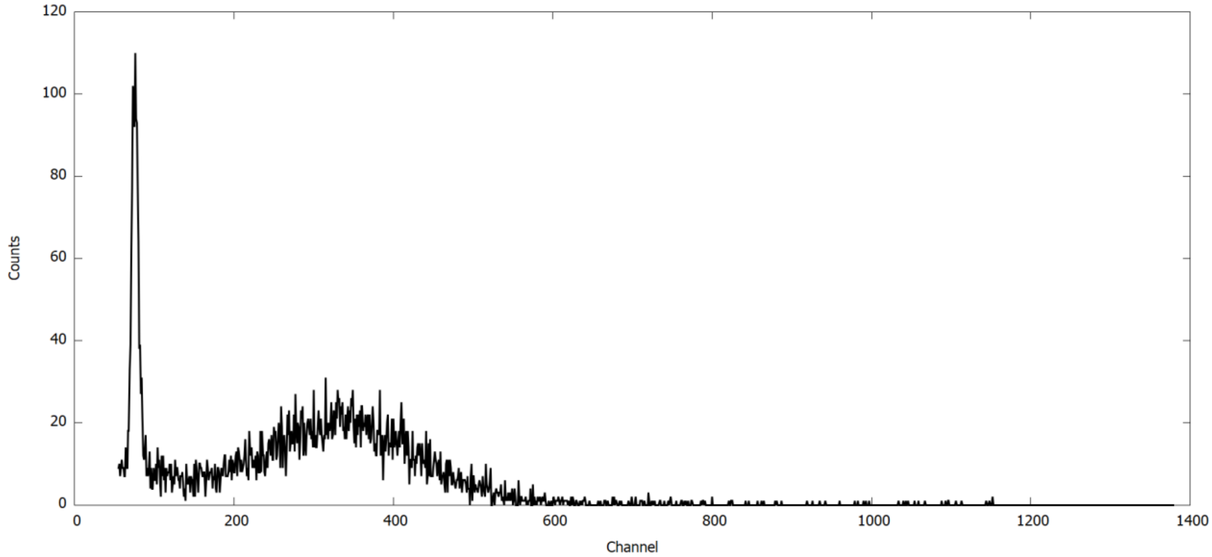

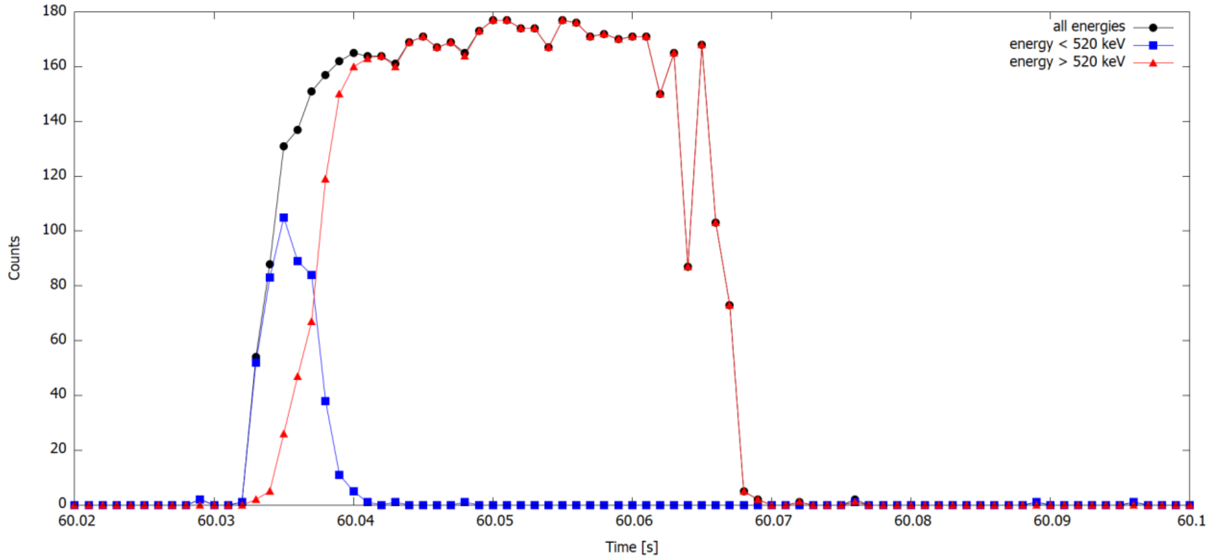

Shot number	**Ip/Bt**	**First gas injection**	**Second gas injection**	**Shape**	**Runaways**	**Comment**
92448	**1.5MA/3T**	**DMV1 7.4 bar 100% Ar**	**DMV2 45bar 100% Kr. t+150ms.**	**Modified Limiter. ID2=ID3=0. IIm=0.0 (with a ramp in 92449)**	**Plateau. 610 kA. 85 ms.**	**Decreased Imbalance.**

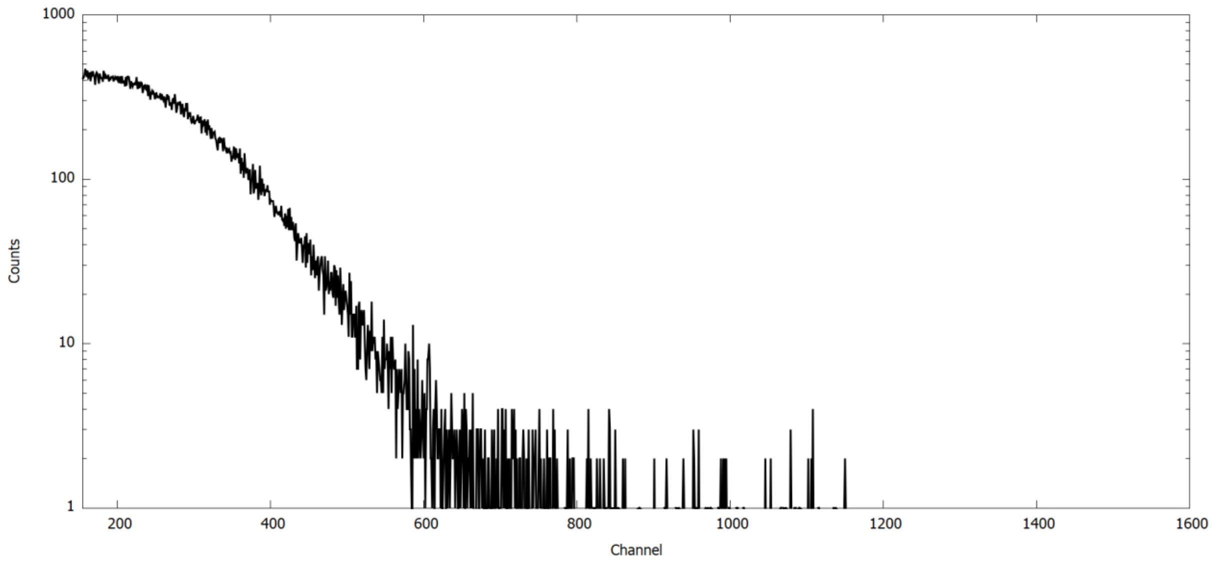

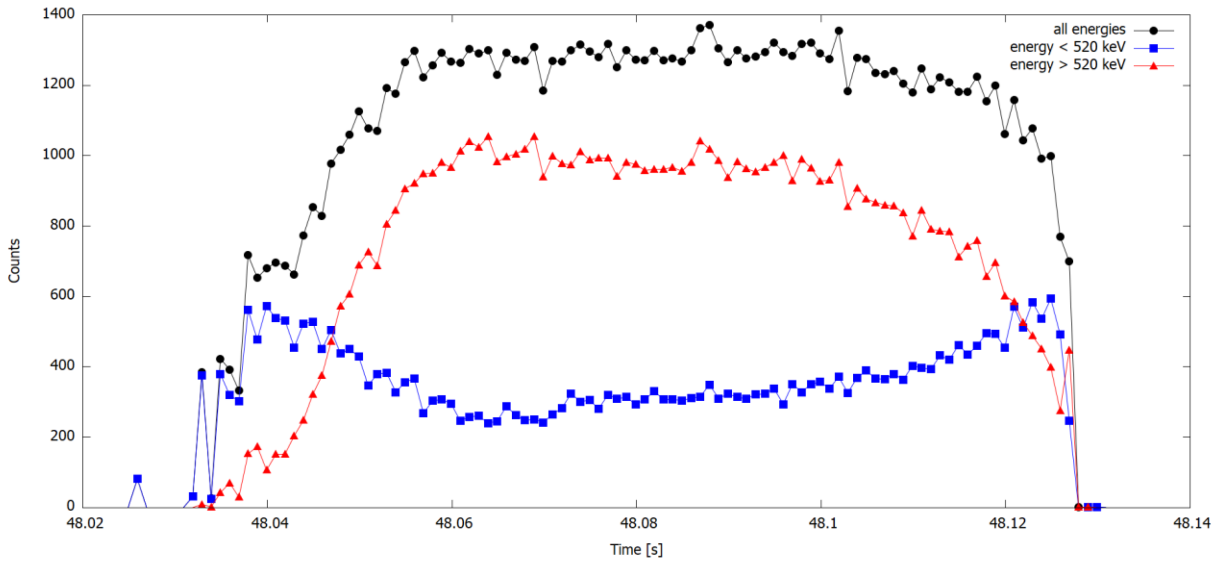

Shot number	Ip/Bt	First gas injection	Second gas injection	Shape	Runaways	Comment
92449	1.5MA/3T	DMV1 7.4 bar 100% Ar	DMV2 45bar 100% Kr. t+150ms.	Modified Limiter. ID2=ID3=0. IIm=0.0 (with a ramp in 92449)	Plateau. 610 kA. 85 ms.	Decreased Imbalance.

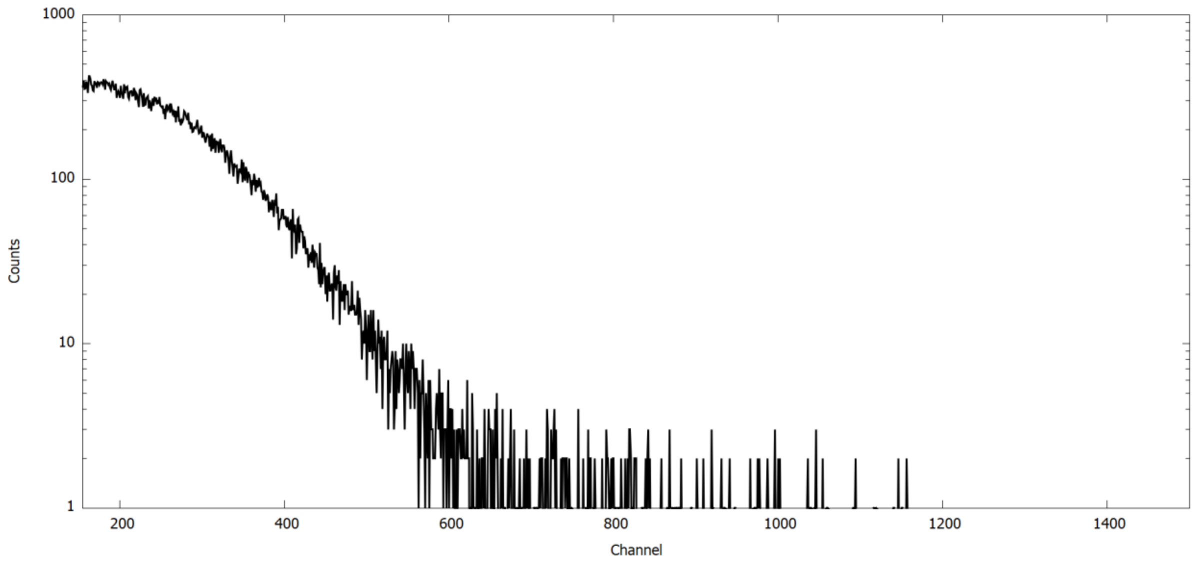

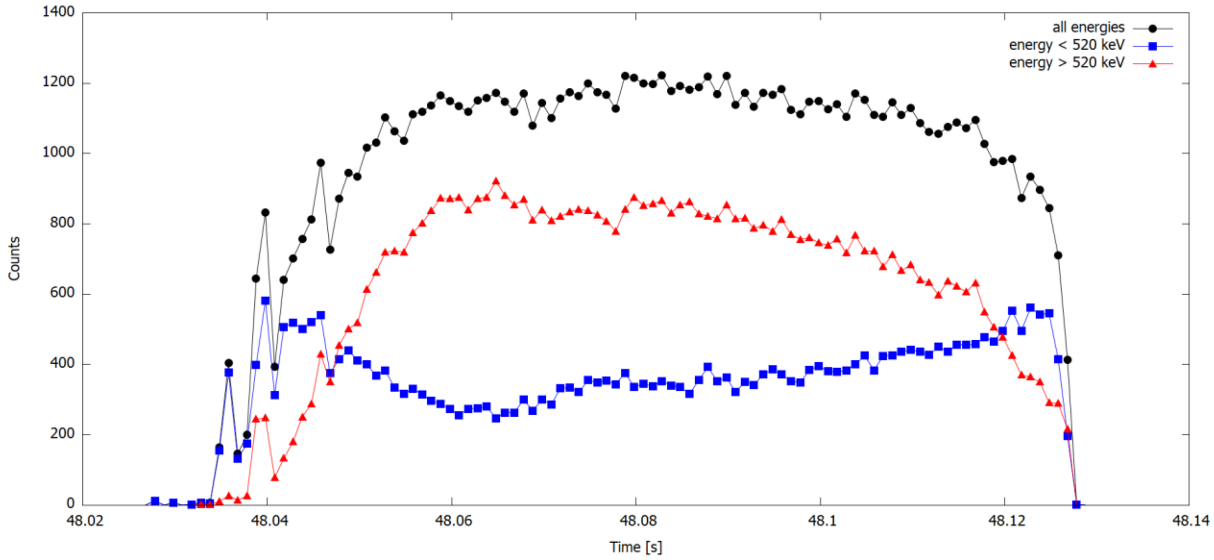

Shot number	Ip/Bt	First gas injection	Second gas injection	Shape	Runaways	Comment
92454	1.5MA/3T	DMV3 1.3 bar 100% Ar	DMV2 45bar 100% Kr. t+150ms.	Modified Limiter. ID2=ID3=0. IIm=0.0	Plateau. 670-720 kA. 105 ms.	DMV3-triggered beam. Late (or not at all) mitigation.

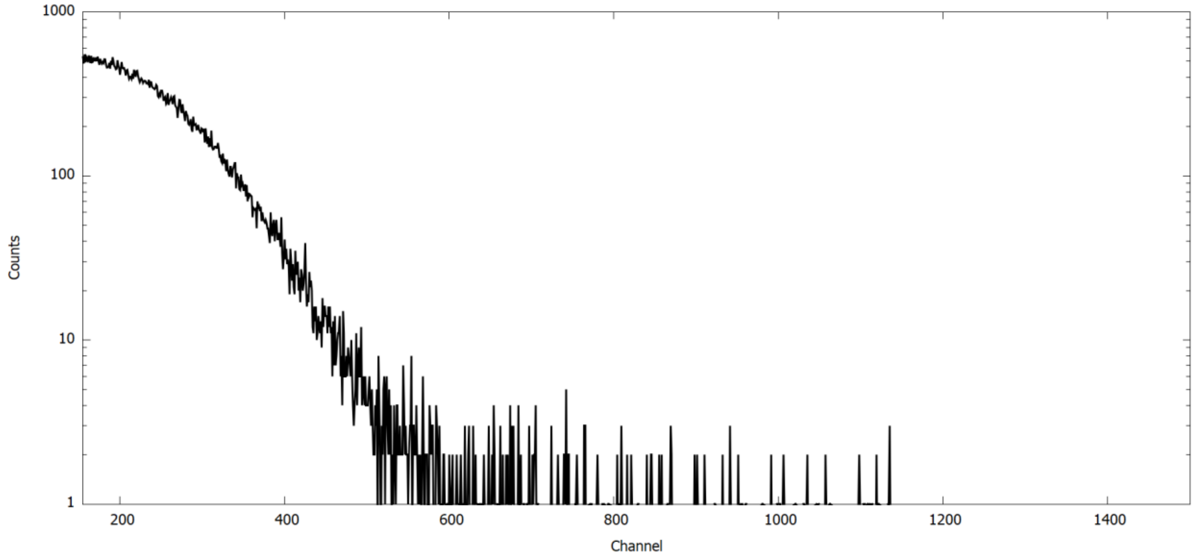

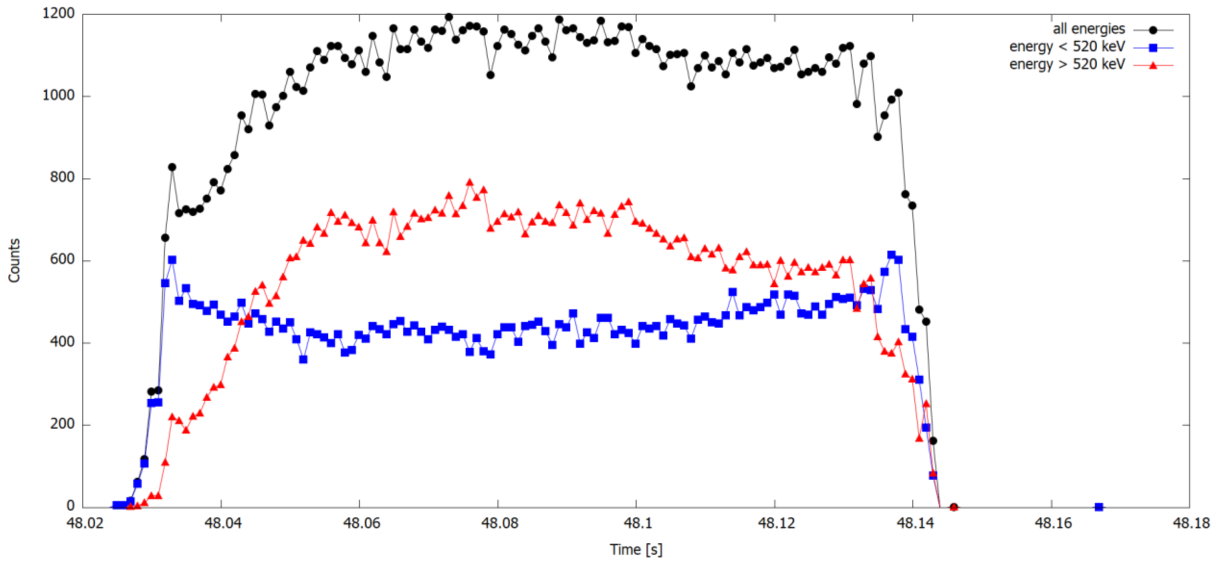

Shot number	**Ip/Bt**	**First gas injection**	**Second gas injection**	**Shape**	**Runaways**	**Comment**
92456	**1.5MA/3T**	**DMV3 1.3 bar 100% Ar**	**DMV2 45bar 100% Kr. t+20ms.**	**Modified Limiter. ID2=ID3=0. IIm=0.0**	**Plateau. 670-720 kA. 105 ms.**	**DMV3-triggered beam. Early mitigation.**

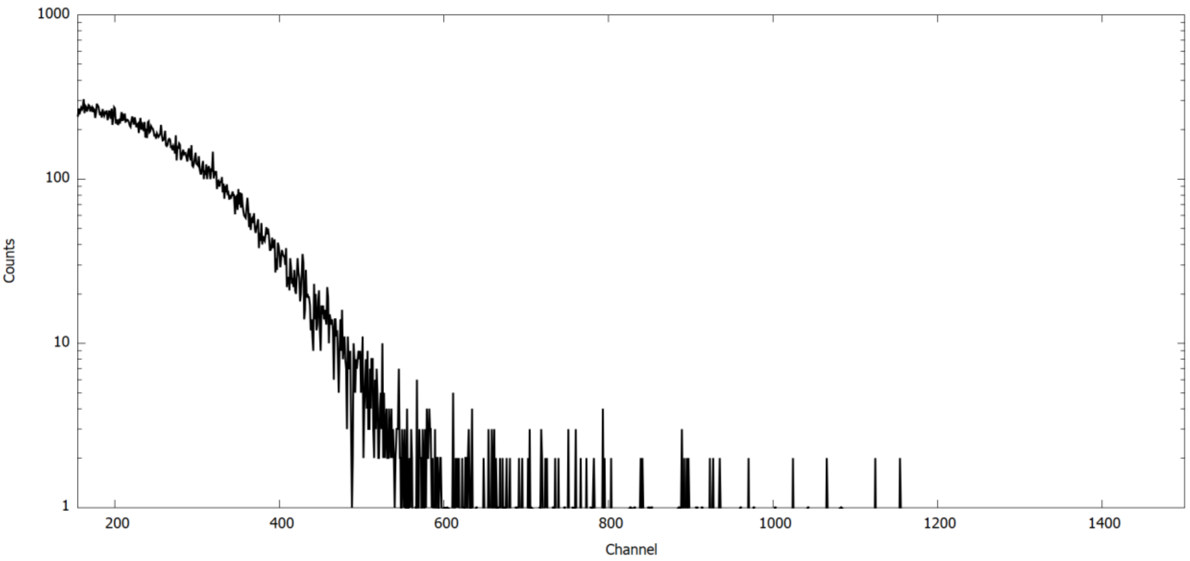

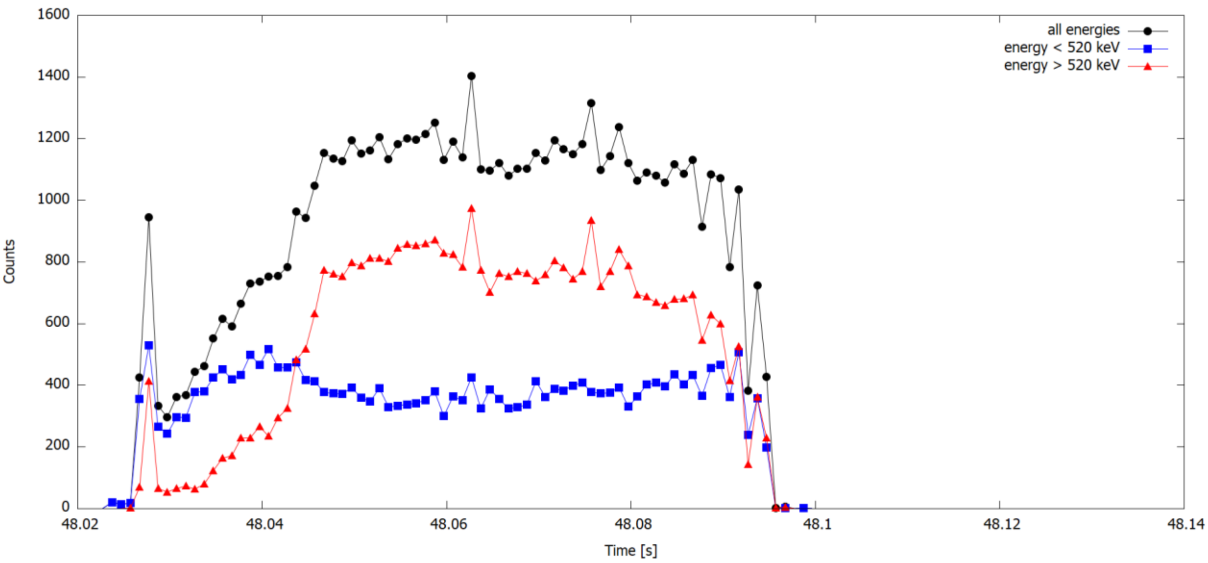

Shot number	Ip/Bt	First gas injection	Second gas injection	Shape	Runaways	Comment
92457	1.5MA/3T	DMV3 1.3 bar 100% Ar	DMV2 45bar 100% Kr. t+20ms.	Modified Limiter. ID2=ID3=0. IIm=0.0	Plateau. 670-720 kA. 105 ms.	DMV3-triggered beam. Early mitigation.

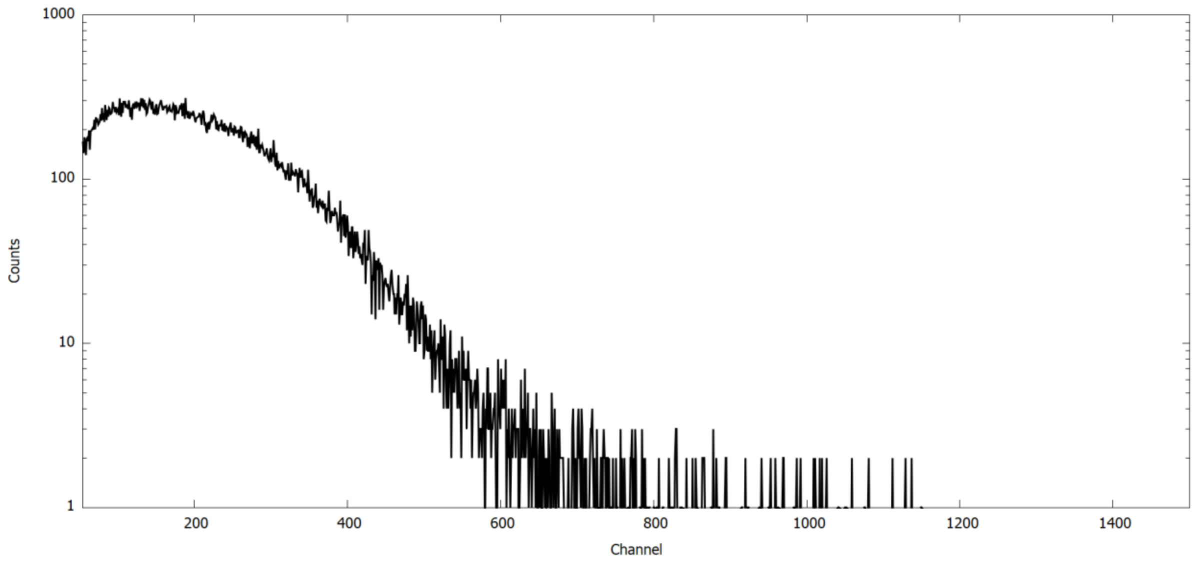

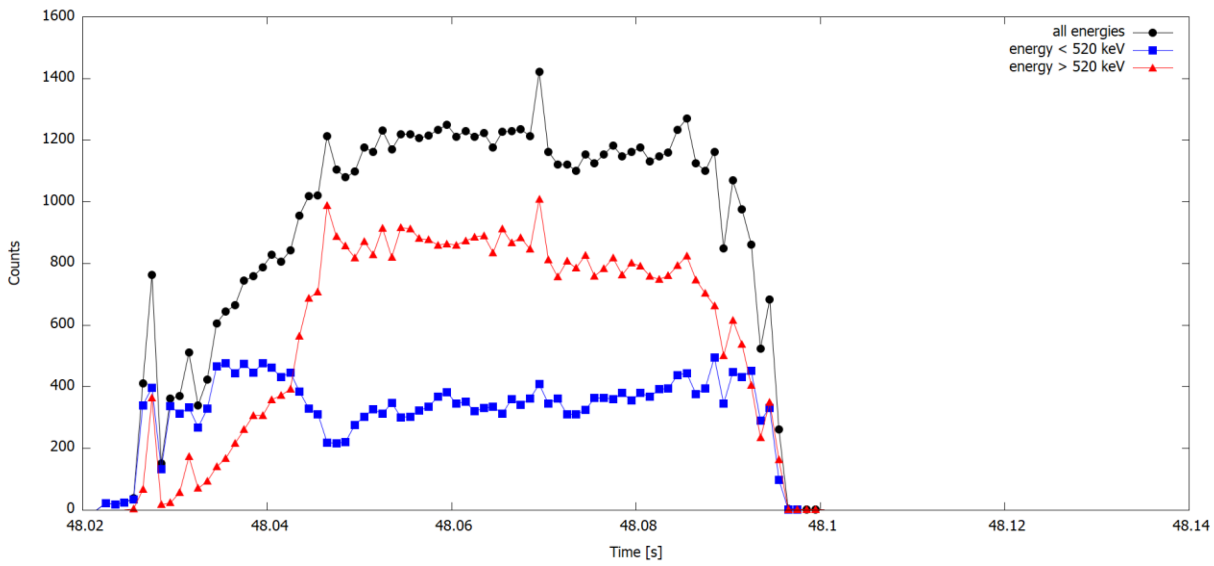

Shot number	Ip/Bt	First gas injection	Second gas injection	Shape	Runaways	Comment
92458	1.5MA/3T	DMV3 1.3 bar 100% Ar	DMV2 45bar 100% Kr. t+150ms.	Modified Limiter. ID2=ID3=0. IIm=0.0	Plateau. 670-720 kA. 105 ms.	DMV3-triggered beam. Late (or not at all) mitigation.

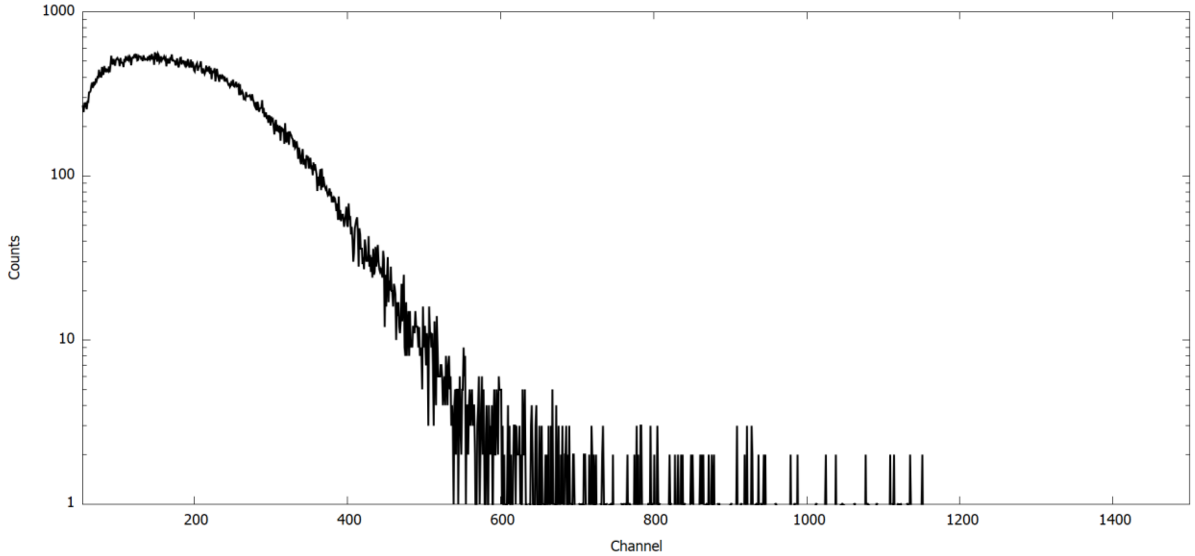

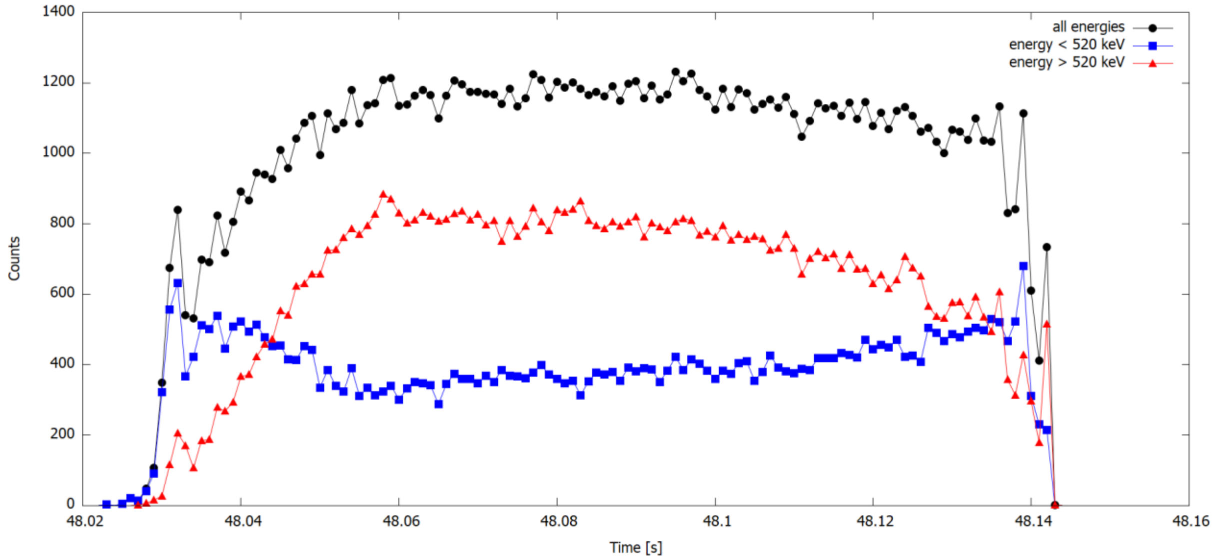

Shot number	Ip/Bt	First gas injection	Second gas injection	Shape	Runaways	Comment
92459	1.5MA/3T	DMV3 0.24 bar 100% Ar	DMV2 45bar 100% Kr. t+200ms.	Modified Limiter. ID2=ID3=0. IIm=0.0	Plateau. 670-720 kA. 105 ms.	DMV3-triggered beam, very low pressure. Late mitigation.

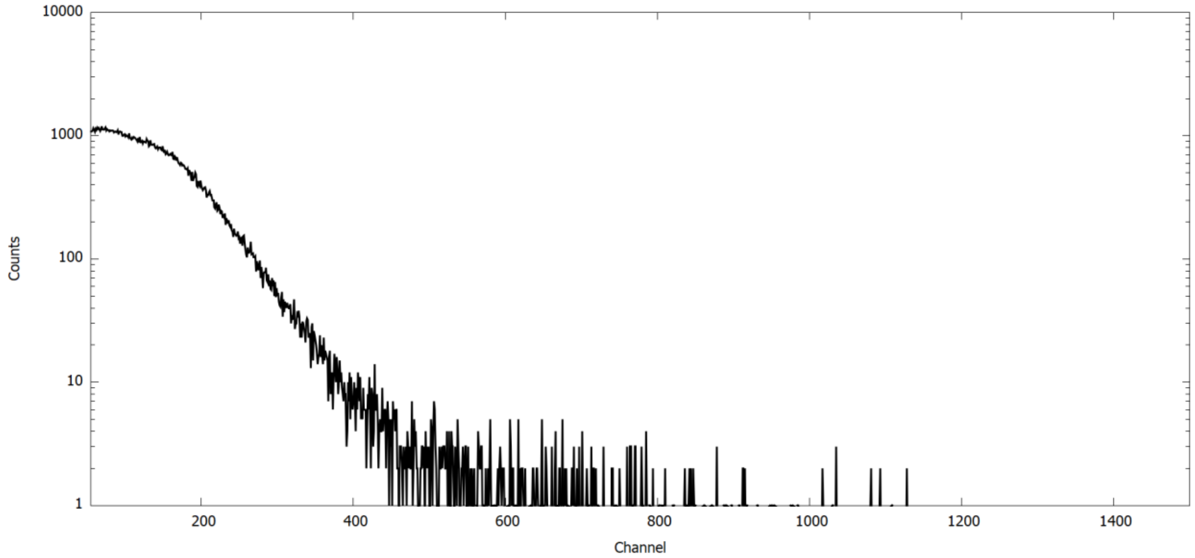

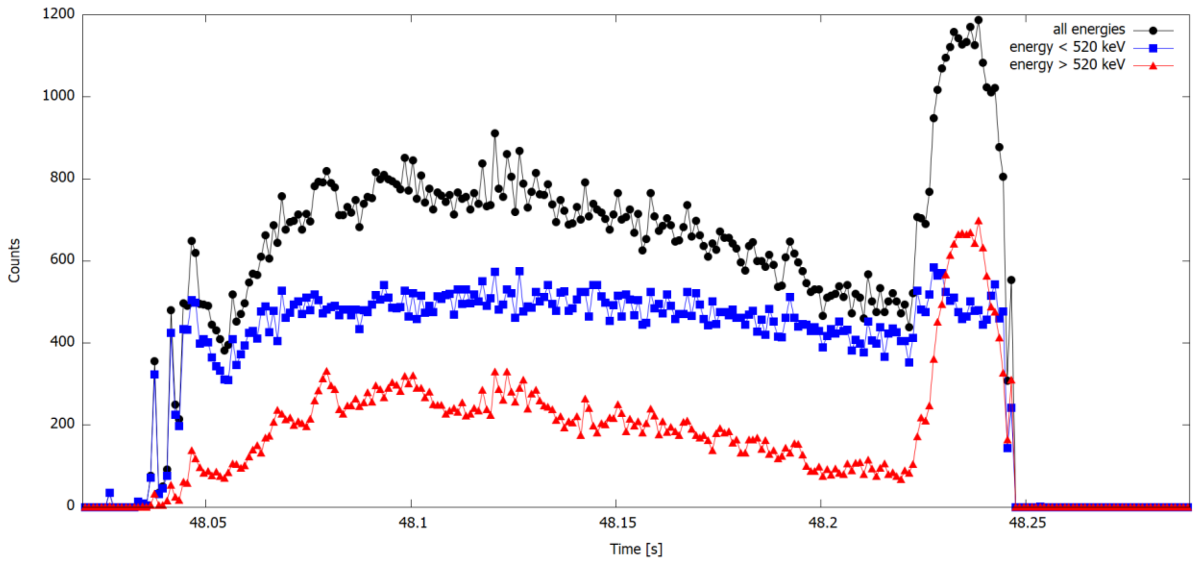

Shot number	Ip/Bt	First gas injection	Second gas injection	Shape	Runaways	Comment
92460	1.5MA/3T	DMV3 0.24 bar 100% Ar	DMV2 45bar 100% Kr. t+30ms.	Modified Limiter. ID2=ID3=0. IIm=0.0	Plateau. 670-720 kA. 105 ms.	DMV3-triggered beam, very low pressure. Early mitigation. Some efficiency ?

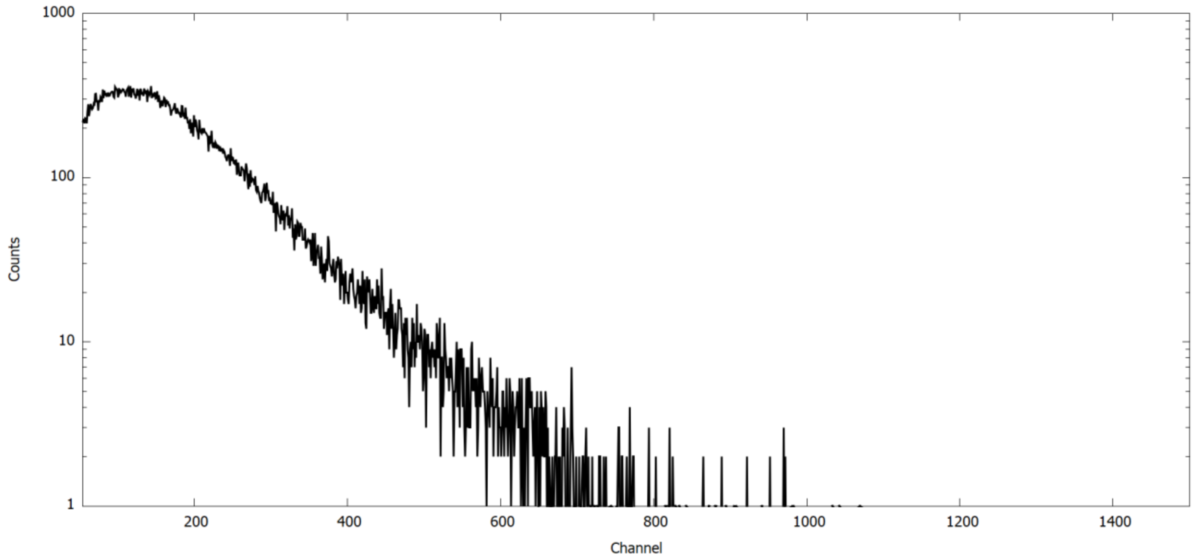

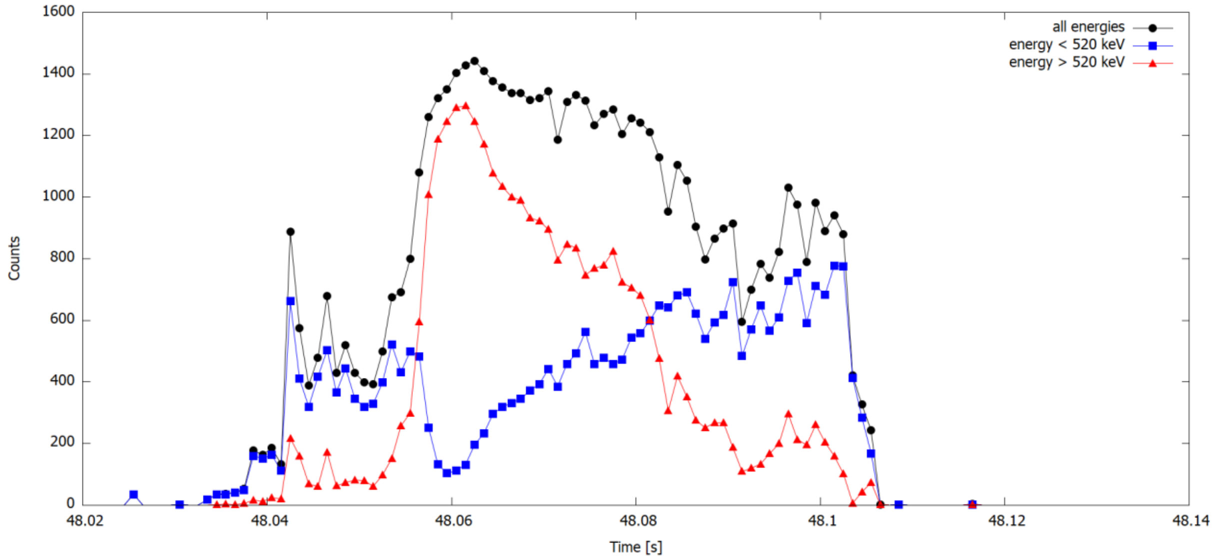

Shot number	Ip/Bt	First gas injection	Second gas injection	Shape	Runaways	Comment
92461	1.5MA/3T	DMV1 7.4 bar 100% Ar	DMV2 45bar 100% Kr. t+30ms + DMV3 39bar 100% Kr	Modified Limiter. ID2=ID3=0. IIm=0.0	Plateau. 670-720 kA. 105 ms.	The full blast (DMV2+DMV3 mitigation).

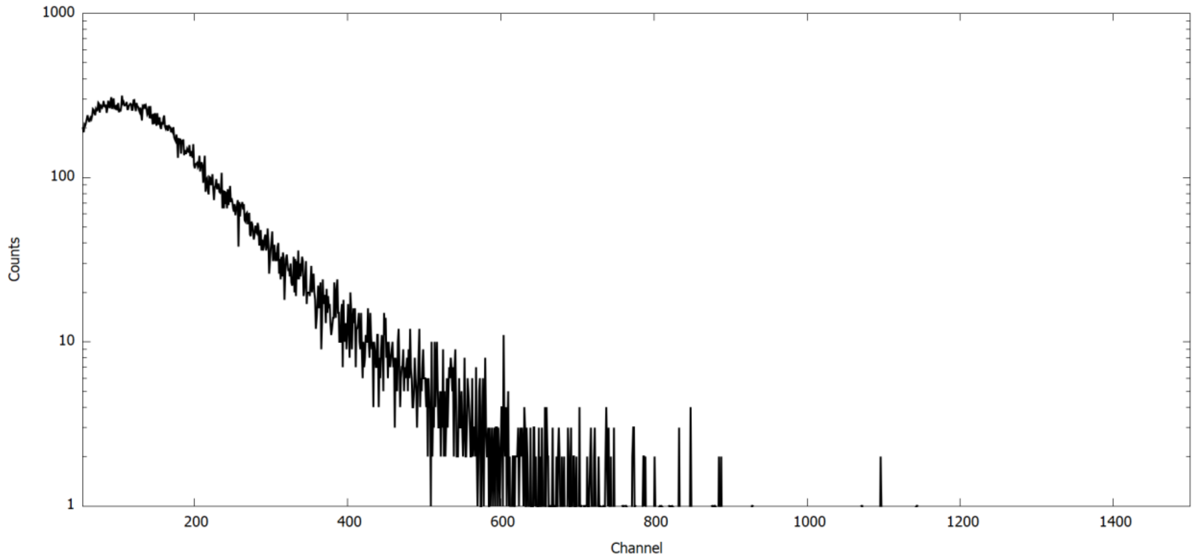

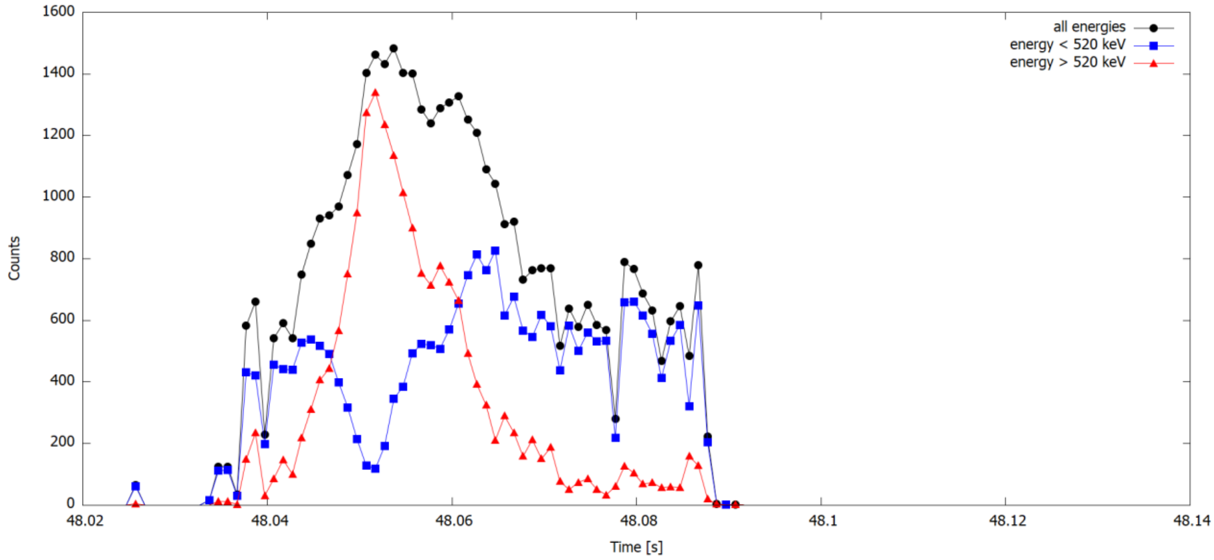

Narodowe Centrum Badań Jądrowych
National Centre for Nuclear Research
ŚWIERK

The report was prepared by the NCBJ team

Arkadiusz Urban, Andrzej Broslawski and Izabella Zychor.

This scientific work was partly supported by Polish Ministry of Science and Higher Education within the framework of the scientific financial resources in the years 2015-2018 allocated for the realization of the international co-financed project.

This work has been carried out within the framework of the EUROfusion Consortium and has received funding from the Euratom research and training programme 2014-2018 under grant agreement No 633053. The views and opinions expressed herein do not necessarily reflect those of the European Commission.